Vol. 16. No.3
ISSN 2477-6041 articles 9, pp. 1125 – 1153, 2025

COMPARATIVE STUDY OF HYPERELASTIC MODELS FOR THERMOPLASTIC ELASTOMERS IN SOFT ROBOTICS

Melsiani R F Saduk [1] 🖂, Edwin P D Hattu[1], Jhon A Wabang [1], Duran Hore [1], Nasaruddin [1], Antonius Pangalinan[1]

[1] **Jurusan Teknik Mesin,**
Politeknik Negeri Kupang
Jl. Adi Sucipto Po Box.139 Penfui
Kupang, NTT, 85148, INDONESIA
melsianisd@gmail.com
edwinhattu10@gmail.com
jhonarwabang@gmail.com
yolanyoel68@gmail.com
nasarkupang@gmail.com
Antoniuspangalinan74@gmail.com

Abstract

The accurate prediction of mechanical behavior in thermoplastic elastomers (TPEs) is essential for improving the performance of soft robotic grippers. This study presents a comparative evaluation of three hyperelastic models—Neo-Hookean, second-order Yeoh, and first-order Ogden—applied to NinjaFlex (TPU), Filaflex (TPE), and Pebax (PEBA). Finite Element Analysis (FEA) was conducted in ANSYS to assess total deformation, equivalent strain, and von Mises stress under internal pressures of 0.08–0.30 MPa. The Yeoh model captured the large-strain behavior in flexible materials, while the Ogden model provided balanced predictions across various stiffness levels. Neo-Hookean served as a computationally efficient baseline but showed limited accuracy under high strain. These findings provide a simulation-based framework for material–model selection in soft robotics and highlight the importance of model–material compatibility in design.

Keywords: *Soft Gripper, Thermoplastic Elastomers, Hyperelastic Material Model, Finite Element Analysis, Deformation Behavior.*

1. INTRODUCTION

Soft robotics has emerged as a rapidly evolving field that leverages the compliant characteristics of soft materials to enable safe and adaptive interaction in unstructured environments [1–3]. In contrast to conventional rigid-body systems, soft robotic platforms utilize elastomeric materials capable of undergoing large elastic deformations, making thermoplastic elastomers (TPE) promising due to their reversible strain behavior and compatibility with additive manufacturing technologies [4–8].

Among the available TPE, materials such as NinjaFlex (TPU), Filaflex (TPE), and Pebax (PEBA) have received considerable attention for their diverse mechanical characteristics—ranging from highly flexible to moderately rigid structures [9–12]. These materials are widely used in components including soft actuators, robotic grippers, and wearable devices, where mechanical compliance, durability, and consistent material performance underload are essential. Nevertheless, accurately predicting their mechanical response under conditions of large deformation remains a significant challenge, primarily due to the non-linear stress–strain behavior inherent in elastomeric materials and the dependency on constitutive model selection [13–15].

Hyperelastic constitutive models such as Neo-Hookean, Yeoh (second-order), and Ogden (first-order) are widely employed in computational mechanics to represent the non-linear elastic behavior of elastomers [16–18]. The Neo-Hookean model is known for

Corresponding Author:
🖂 **Melsiani R F Saduk**
Received on: 2025-05-13
Revised on: 2025-07-23
Accepted on: 2025-12-01

DOI: 10.21776/jrm.v16i3.2122

its simplicity and numerical stability; however, it is often insufficient for accurately representing large-strain responses. In contrast, Yeoh and Ogden offer greater flexibility in capturing complex deformation behavior; however, these models demand more detailed parameter calibration and involve increased computational effort.

In parallel, various studies have attempted to tailor the mechanical behavior of TPEs through printing parameter optimization—such as nozzle temperature, layer height, and printing orientation—to enhance model fidelity. However, these efforts have often lacked a systematic approach in selecting constitutive models, making it difficult to generalize findings across materials and printing setups. Given that design engineers frequently rely on simulation results during the conceptual phase, establishing a clear benchmark for material-model compatibility becomes essential. These benchmarks must not only ensure theoretical accuracy but also address the manufacturing constraints inherent in additive manufacturing workflows.

Despite the growing application of these models in soft robotics, comprehensive comparative studies across commercial TPEs remain limited. Prior research has predominantly focused on individual materials or employed only one or two constitutive models—for instance, the Ogden model has frequently been applied to NinjaFlex [19,20], while the Yeoh model has been used for PEBA and other TPU-based structures [21,22]. In many cases, simulations rely on a single hyperelastic model for the sake of simplicity, despite its limited capability in capturing the full spectrum of large deformation behavior [23,24]. Furthermore, the application of hyperelastic models to 3D-printed TPE structures is complicated by fabrication-induced inconsistencies including issues like anisotropy, residual stresses, and interlayer delamination. These issues arise due to the layer-by-layer deposition process inherent in fused deposition modeling (FDM), which affects the material's stress–strain response in a directionally dependent manner. As a result, models including Neo-Hookean may oversimplify deformation behavior, while Ogden and Yeoh, although more flexible, demand detailed calibration that is rarely feasible in practical applications. This mismatch between real-world printed behavior and idealized model assumptions further underscores the necessity for a systematic comparison of model–material performance in simulation environments.

This research aims to address this gap by evaluating the predictive capabilities of the hyperelastic models applied to three different TPEs using FEA in ANSYS. Simulations were conducted under internal pressure levels ranging from 0.08 to 0.30 MPa to assess total deformation, equivalent strain, and von Mises stress responses. The outcomes are correlated with the intrinsic material properties of stiffness and extensibility, thereby providing guidance for rational material–model selection in the context of soft robotic component design. Ultimately, this study contributes a novel comparative dataset that informs design optimization and model calibration strategies for next-generation soft actuators.

2. MATERIAL AND METHODS

In the development of soft robotic systems, material selection plays a pivotal role in determining performance, flexibility, and overall functionality. The choice of material for a soft actuator directly influences its ability to undergo deformation while maintaining structural integrity, which is critical for tasks such as gripping, bending, and adapting to various surfaces. This study focuses on three widely used thermoplastic elastomers (TPE), known for their capacity to endure large elastic deformations and stable recovery under repeated loading conditions. The following sections detail the materials selected for this study, along with the methods used to characterize their mechanical properties and the simulations conducted.

2.1 Materials Selection

This study selected three commercially available TPE that are commonly utilized in soft robotic systems due to their capacity for large elastic deformation and stable recovery: NinjaFlex (TPU), Filaflex (TPE), and Pebax (PEBA). These materials exhibit distinct mechanical properties, particularly in stiffness, density, and strength (see Table 1).

2.2 Data Collection

The mechanical properties applied in simulations were obtained from manufacturer datasheets and validated sources in the literature[25–29]. Table 1 outlines the key mechanical properties for the selected materials, including their density, Young's modulus, Poisson's ratio, shear modulus, and tensile strength

Table 1. Mechanical Properties of the Materials.

PROPERTIES	Hyperelastic Materials		
	NinjaFlex	Filaflex	PEBA
Density (g/cm³)	1.2	1.05	1.14
Young's Modulus (MPa)	25	10	60
Poisson's Ratio	0.47	0.45	0.41
Shear Modulus (MPa)	3.5	2.0	50
Tensile Ultimate Strength (MPa)	30	15	45

2.3 Hyperelastic Material Modeling

Three hyperelastic constitutive models were employed to characterize the non-linear elastic behavior of the selected TPEs: Neo-Hookean, Yeoh model, and Ogden model, as described in Equations (1), (2), and (3), respectively. Each model defines the strain energy potential W in terms of deformation invariants or principal stretches, depending on the model formulation.

Neo-Hookean[30]:

$$W = \mu(I_1 - 3) \tag{1}$$

where μ is the shear modulus and I_1 is the first invariant of the Cauchy-Green tensor.

Yeoh model [31]:

$$W = C_1(I_1 - 3) + C_2(I_1 - 3)^2 \tag{2}$$

with C1 and C2 are material constants derived through curve fitting to experimental data

Ogden model [32]

$$W = \frac{\mu_1}{\alpha_1}\left(\lambda_1^{\alpha_1} + \lambda_2^{\alpha_1} + \lambda_3^{\alpha_1} - 3\right) \tag{3}$$

Where, λi denotes principal stretch, and μ1, α1 are fitting parameters based on non-linear regression.

2.4 Data Processing

The collected mechanical data was incorporated into hyperelastic constitutive models and processed through FEA) in ANSYS Workbench. Each simulation used consistent meshing and loading conditions to ensure comparability among material–model combinations.

2.5 CAD Model Design

A 3D model of a soft robotic gripper finger was designed using CAD software, with dimensions 168 mm × 15 mm × 24 mm. This geometry was imported into ANSYS

Workbench for meshing and simulation. A uniform tetrahedral mesh size of 1 mm was used, based on convergence testing for computational efficiency and result stability.

The detailed dimensional design of the soft gripper, including sectional view and geometric layout, is presented in Figure 1.

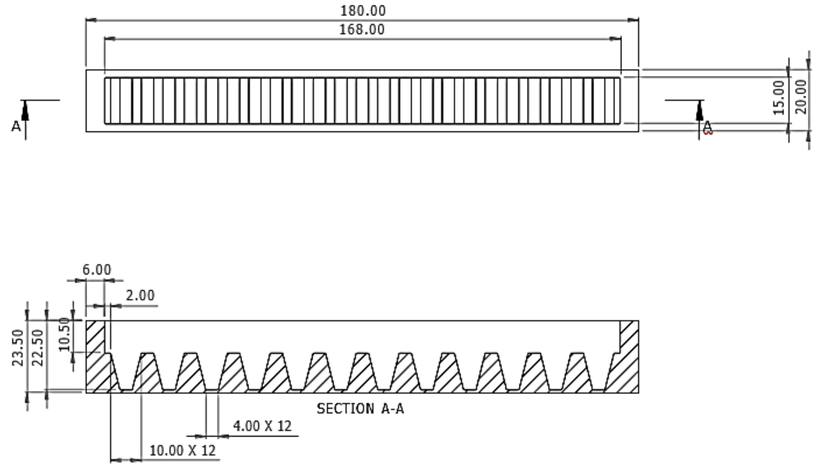

Figure 1. Design of the soft gripper used for hyperelastic simulation, including top view and sectional profile (A–A)

2.6 Finite Element Analysis Set Up

The simulations were conducted in ANSYS under three internal pressure levels 0.08 MPa, 0.10 MPa, and 0.30 MPa—which reflect realistic actuation intensities typically encountered in soft robotic applications. The base of the gripper finger was fixed, while gravitational acceleration (9.81 m/s²) was applied in the negative Y-direction. All simulations assumed a static, isothermal condition with no thermal coupling or dynamic effects considered.

The workflow of the hyperelastic simulation process in ANSYS Workbench is illustrated in Figure 2, which illustrates the following:

(a) the applied boundary conditions and loading configuration, and

(b) the meshing scheme employed for the soft robotic gripper model.

These configurations ensure accurate deformation capture and maintain solution convergence under non-linear loading conditions.

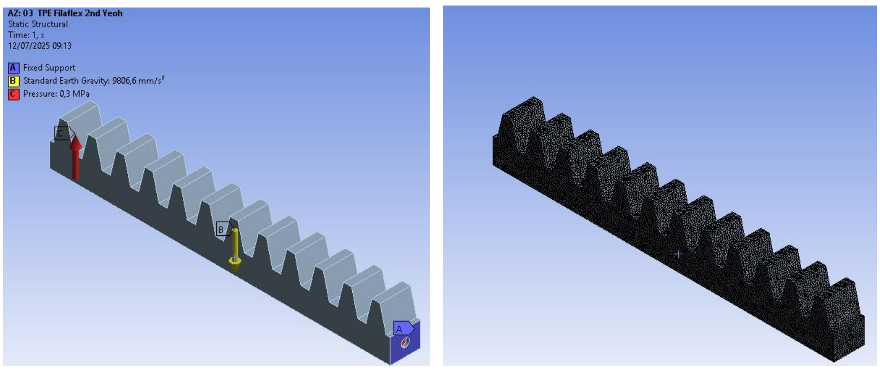

(a) **(b)**

Figure 2. Hyperelastic simulation setup in ANSYS Workbench: (a) boundary conditions and applied loading; (b) meshing configuration implemented for the gripper model.

2.7 Algorithm and Program

The simulation workflow for hyperelastic material modeling in ANSYS Workbench follows a structured sequence to ensure consistency and comparability among different materials and constitutive models. As shown in Figure 4, the process begins with the definition of boundary conditions, pressure levels, and simulation environment.

The 3D CAD model of the soft gripper is then imported into ANSYS. For each material—NinjaFlex, Filaflex, and PEBA—hyperelastic properties are assigned according to the selected model: Neo-Hookean, Yeoh, or Ogden. Meshing is performed using tetrahedral elements with a mesh size of 1 mm, as validated through convergence testing.

Subsequently, boundary conditions and internal pressure loads are applied, and static structural simulations are conducted under isothermal assumptions. The simulation outputs include total deformation, equivalent elastic strain, and von Mises stress. This systematic algorithm ensures repeatability, numerical stability, and meaningful comparative analysis between material–model combinations.

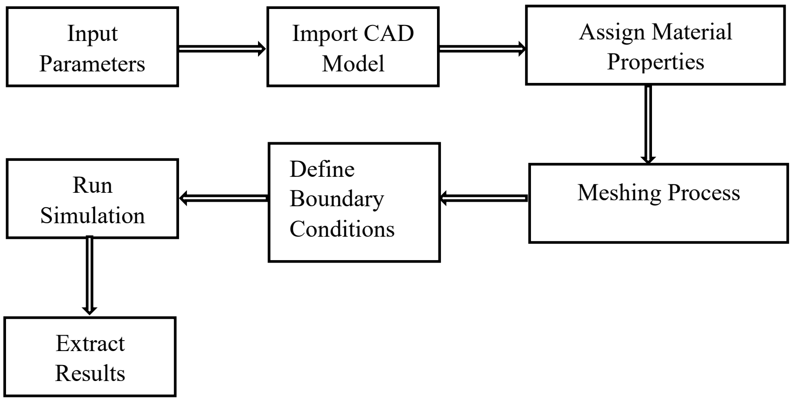

Figure 3. Simulation workflow for hyperelastic analysis in ANSYS Workbench.

2.8 Key Performance Metrics

The simulation outputs were evaluated using three main performance metrics:

Total Deformation (δ): Maximum displacement recorded at the gripper tip, indicating flexibility.

Equivalent Strain (ε_eq): A scalar value representing strain intensity within the structure.

$$\varepsilon_{eq} = \sqrt{\frac{2}{3}[(\varepsilon_1 - \varepsilon_2)^2 + (\varepsilon_2 - \varepsilon_3)^2 + (\varepsilon_3 - \varepsilon_1)^2]} \quad (4)$$

Von Mises Stress (σ_eq): A derived scalar stress used to assess material yield risk under multiaxial loading.

$$\sigma_{eq} = \sqrt{\frac{1}{2}[(\sigma_1 - \sigma_2)^2 + (\sigma_2 - \sigma_3)^2 + (\sigma_3 - \sigma_1)^2]} \quad (5)$$

These indicators provide a comprehensive representation of material response under simulated actuation, enabling both qualitative and quantitative comparisons between models and materials.

3. RESULTS AND DISCUSSION

3.1 Analysis of Individual Material Responses

NinjaFlex (TPU)

NinjaFlex (TPU) exhibited a consistent and stable deformation response under varying internal pressures. Finite element simulations were conducted at three internal pressures: 0.08 MPa, 0.10 MPa, and 0.30 MPa, using three hyperelastic material models: Neo-Hookean, Yeoh, and Ogden. These models, though differing in mathematical formulation, were calibrated using the same mechanical properties obtained from material characterization (see Table 1), including Young's modulus, Poisson's ratio, shear modulus, and tensile strength. This consistent input ensures that the deformation behavior reflects the material's inherent characteristics rather than differences in the model structure.

The results demonstrated a nonlinear yet progressive trend in deformation, confirming NinjaFlex's ability to withstand large elastic strains while maintaining mechanical stability—critical for soft robotic applications requiring adaptive deformation. The consistent behavior of NinjaFlex under these varying loading conditions is corroborated by previous studies [33], which analyzed the material's mechanical properties and confirmed its stable deformation under different pressure levels. Similar findings were reported in the context of pneumatic actuators [34,35]**.** Moreover, the tunable stiffness of TPU under compressive forces has also been demonstrated [36], further supporting its suitability for applications involving variable mechanical loads.

At 0.30 MPa, the maximum displacement reached 159.8 mm, indicating that NinjaFlex can undergo substantial deformation without losing structural integrity. At the lower pressures of 0.08 MPa and 0.10 MPa, the displacements recorded were 84.3 mm and 118.5 mm, respectively. These findings suggest that NinjaFlex can withstand significant elastic strains, confirming its suitability for use in flexible, high-deformation soft robotic system [37-39].

The simulation results at 0.30 MPa using the Neo-Hookean model are presented in Figure 4. Panel (a) of the figure indicates that the total deformation is concentrated near the fingertip, with the maximum displacement of 159.8 mm. Panel (b) reveals the equivalent elastic strain, which is uniformly distributed along the gripper with a peak value of 0.6239 mm/mm, indicating that the material deforms evenly without strain localization. In panel (c), the von Mises stress is shown, with a peak of 6.84 MPa at the mid-joint curvature—well within safe limits for the material—demonstrating that NinjaFlex can absorb internal stress effectively without failure.

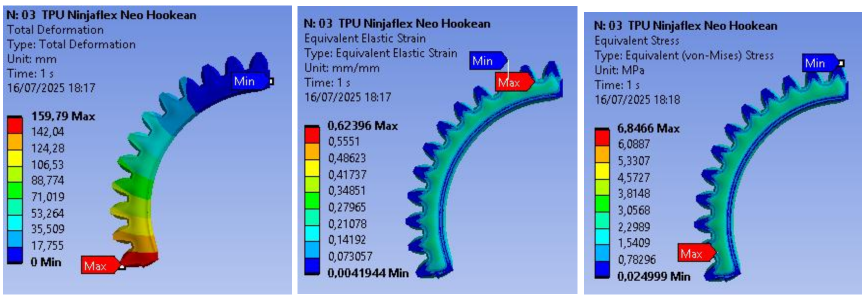

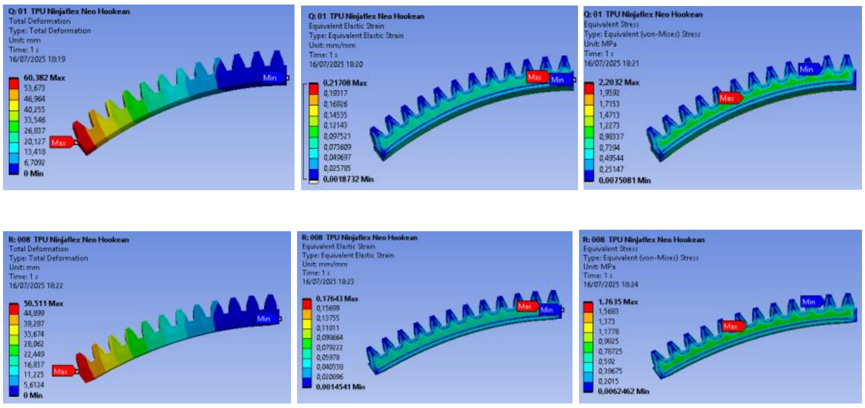

(a) (b) (c)

Figure 4. ANSYS simulation results using Neo-Hookean. The image illustrates total deformation (a), equivalent elastic strain (b), and equivalent von-Mises stress (c)

In the results shown in Figure 5, the Yeoh model was applied to simulate the material response at 0.08 MPa, 0.10 MPa, and 0.30 MPa pressures. As with the Neo-Hookean model, the deformation increases progressively with pressure, with the maximum displacement of 159.8 mm observed at 0.30 MPa, 118.5 mm at 0.10 MPa, and 84.3 mm at 0.08 MPa. In panel (a) of the figure, total deformation is demonstrated, indicating that displacement is largest near the fingertip for all pressures. Panel (b) presents the equivalent elastic strain, which remains evenly distributed along the gripper, confirming that NinjaFlex exhibits stable strain performance without excessive concentration. Panel (c) illustrates the von Mises stress, which remains within safe limits and does not exceed 6.84 MPa, reinforcing the material's ability to handle stress under increasing load. These findings are consistent with previous studies [36] that evaluated TPU behavior under compressive loading conditions.

The simulation results for NinjaFlex at all three pressure levels using the Ogden model are shown in Figure 6. Similar to the Neo-Hookean and Yeoh models, the total deformation increases with pressure, reaching 159.8 mm at 0.30 MPa. In panel (a), the displacement is consistently larger at higher pressures, confirming the nonlinear deformation response. Panel (b) illustrates that the equivalent elastic strain remains uniformly distributed across the gripper, with a peak value of 0.6239 mm/mm. Panel (c) demonstrates that the von Mises stress remains stable across pressure levels, with the highest value of 6.84 MPa occurring at the mid-joint, showing that the material can handle high stress without localized failure. This stability under large deformation was also affirmed in prior investigations [40].

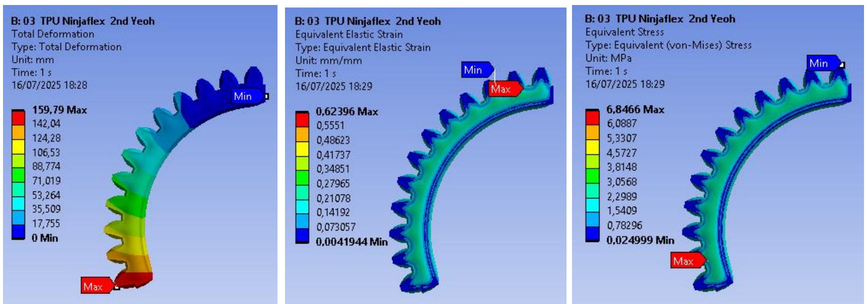

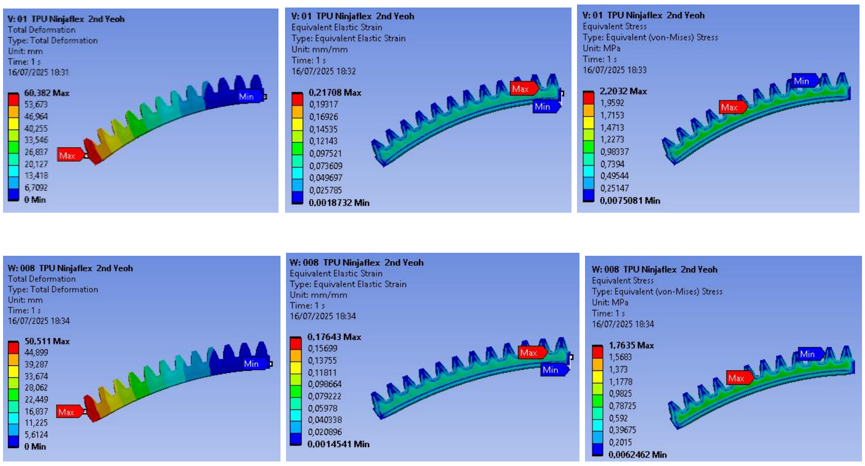

(a) (b) (c)

Figure 5. ANSYS simulation results using the Yeoh model. The image illustrates total deformation (a), equivalent elastic strain (b), and equivalent von-Mises stress (c).

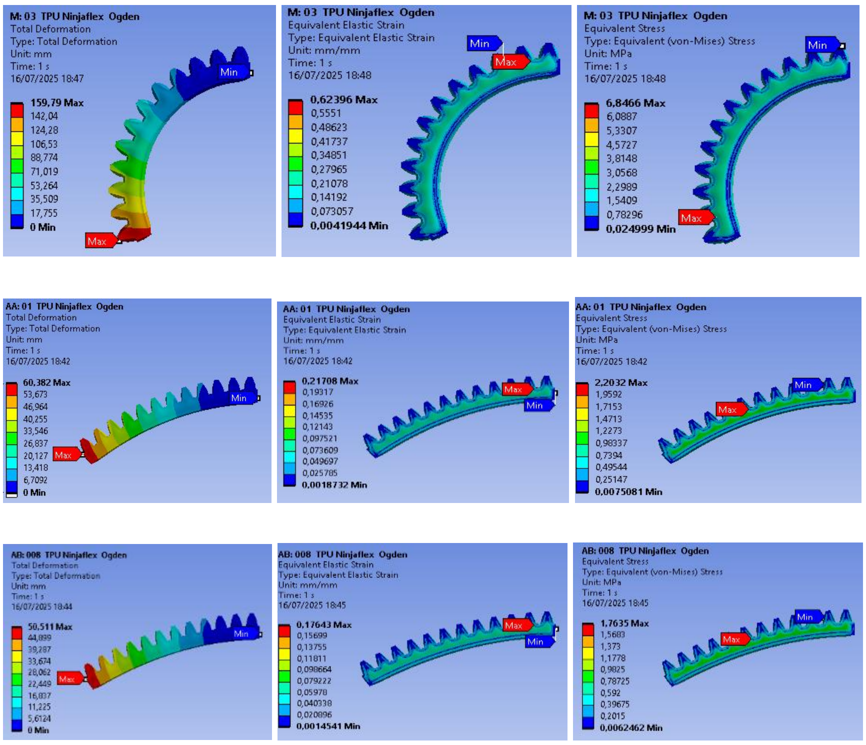

(a) (b) (c)

Figure 6. ANSYS simulation results using the Ogden model. The image illustrates total deformation (a), equivalent elastic strain (b), and equivalent von-Mises stress (c).

In Figure 7, the total deformation of NinjaFlex is compared across the three hyperelastic models (Neo-Hookean, Yeoh, Ogden) under three different pressure levels (0.08 MPa, 0.10 MPa, and 0.30 MPa). The results demonstrate a progressive increase in deformation with increasing pressure, but the values remain closely matched across all three models. This consistency can be attributed to the use of identical mechanical input parameters across the models, allowing for a controlled comparison of model effects. It highlights the model-tolerant nature of NinjaFlex, demonstrating its robustness and confirming its suitability for soft robotic applications where model assumptions may vary. This is consistent with findings from previous studies, which also confirmed model stability for TPU materials in FEM simulations [41,42].

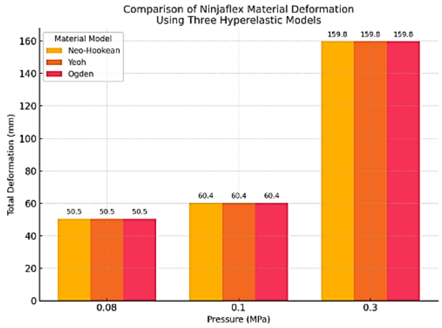

Figure 7. Total deformation of NinjaFlex under three pressure levels.

The results indicate that NinjaFlex (TPU) exhibits consistent deformation, uniform strain distribution, and stable stress handling under varying internal pressures. The material's predictable response across different hyperelastic models—underpinned by uniform calibration—makes it highly suitable for applications in soft robotics, including pneumatic soft grippers, bending actuators, and shape-adaptive robotic interfaces.

Filaflex (TPE)

Filaflex, a thermoplastic elastomer (TPE)-based material, exhibits pronounced nonlinear deformation behavior under varying internal pressures. Finite element simulations were conducted at internal pressures of 0.08 MPa, 0.10 MPa, and 0.30 MPa using three distinct hyperelastic models: Neo-Hookean, Yeoh, and Ogden. Unlike NinjaFlex, the results revealed that Filaflex displays a higher degree of sensitivity to the selected constitutive model, particularly at elevated pressure levels [43-47].

As illustrated in Figure 8, the Neo-Hookean model predicted a maximum deformation of 189.07 mm at 0.30 MPa (panel a), with a peak strain of 0.76355 mm/mm (panel b), and von Mises stress of 7.10 MPa (panel c). This response indicates that Filaflex can undergo large elastic deformation with reasonably uniform stress and strain fields at moderate pressures.

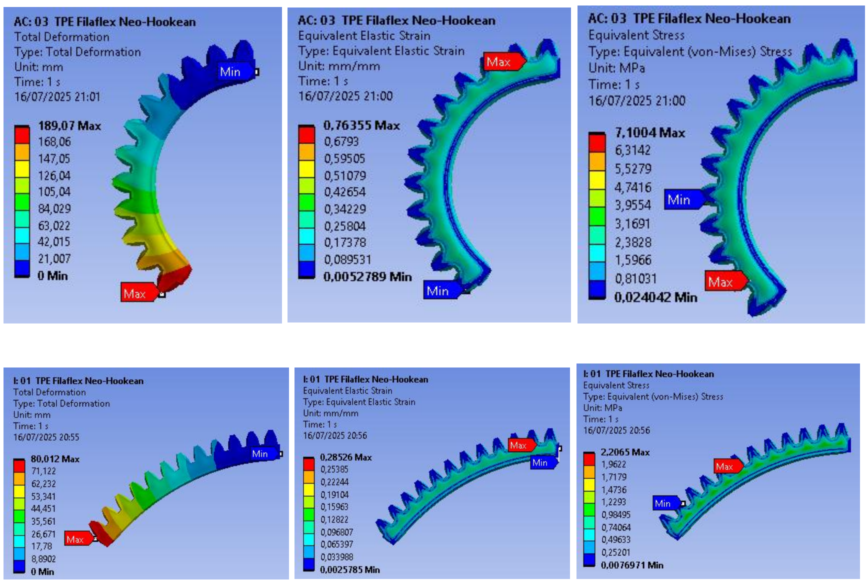

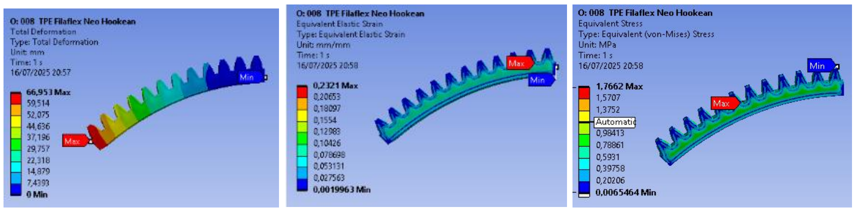

(a) (b) (c)

Figure 8. ANSYS simulation results using the Neo-HookeanModel. The image illustrates total deformation (a), equivalent elastic strain (b), and equivalent von-Mises stress (c).

The Yeoh model, presented in Figure 9, yielded significantly higher deformation, reaching 252.96 mm at 0.30 MPa (panel a). The strain field was more intense (0.92096 mm/mm, panel b), and the peak von Mises stress rose to 19.66 MPa (panel c). These values indicate that the Yeoh model captures the material's high compliance under pressure more aggressively than the Neo-Hookean model. The results align with previous studies asserting that the Yeoh model excels in predicting large-strain behavior in soft elastomers[48-52].

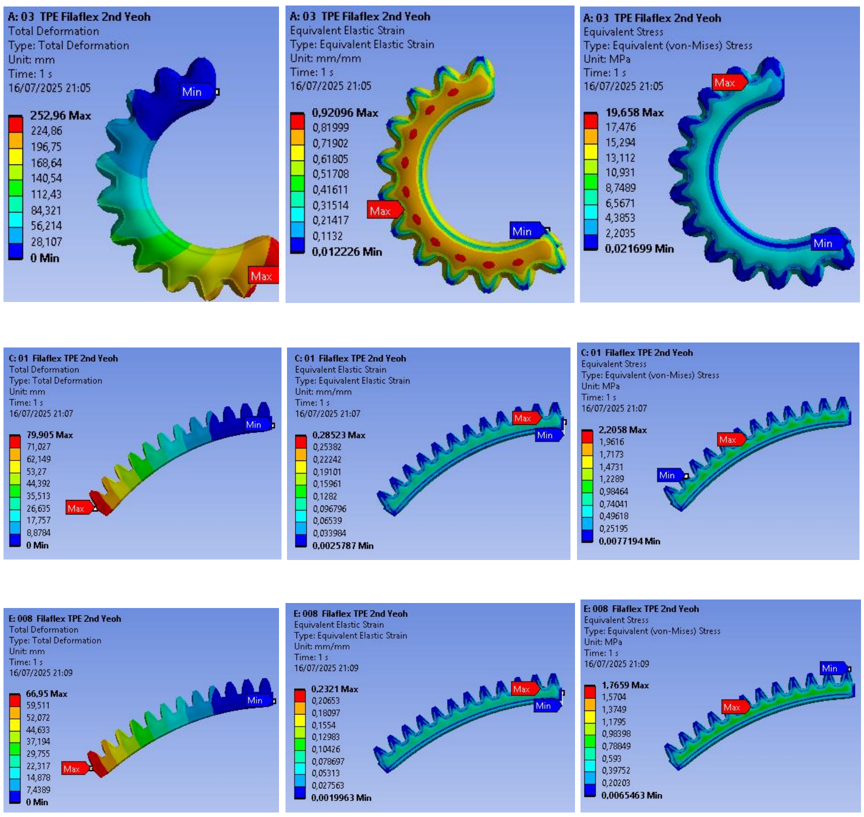

(a) (b) (c)

Figure 9. ANSYS simulation results using the Yeoh model. The image illustrates total deformation (a), equivalent elastic strain (b), and equivalent von-Mises stress (c).

Conversely, the Ogden model in Figure 10 produced a more moderate response. At 0.30 MPa, the deformation was 159.53 mm (panel a), the peak strain was 0.62327 mm/mm (panel b), and the von Mises stress remained at 6.84 MPa (panel c). This model provided a more conservative estimate compared to Yeoh, highlighting the impact of constitutive model formulation on strain energy distribution [43,44], [53].

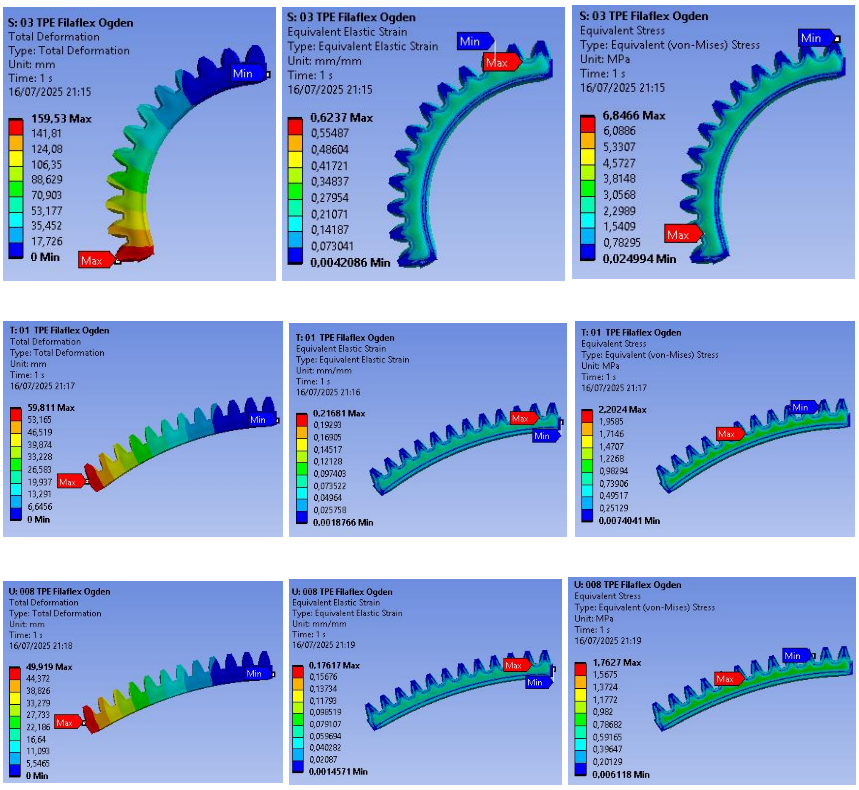

(a) **(b)** **(c)**

Figure 10. ANSYS simulation results using the Ogden model. The image illustrates total deformation (a), equivalent elastic strain (b), and equivalent von-Mises stress (c).

A cross-model comparison is demonstrated in Figure 11, depicting the total deformation at all three pressure levels. At 0.08 MPa, the values ranged from 62 mm (Ogden) to 65 mm (Neo-Hookean and Yeoh). At 0.10 MPa, the deformation varied from 82 mm (Ogden) to 86 mm (Yeoh). However, at 0.30 MPa, the discrepancy became more prominent: 255 mm (Yeoh), 189 mm (Neo-Hookean), and 185 mm (Ogden), confirming the divergence at high strain regimes.

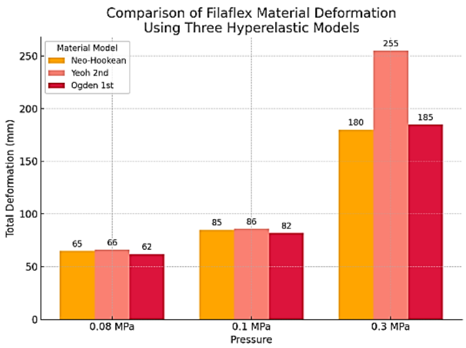

Figure 11. Total deformation of Filaflex under three pressure levels.

This variability can be attributed to Filaflex's low elastic modulus and shear modulus, which make the material particularly sensitive to strain energy formulations. Prior research has indicate that soft materials with shear moduli below 15 MPa are prone to predictive divergence depending on the chosen constitutive model [45, 46], [54]

Thus, while Filaflex demonstrates high compliance and the capacity for large elastic deformation, accurate simulation of its behavior requires careful model selection. Among the tested models, the Yeoh model consistently provided more accurate and stable predictions for large deformation scenarios, making it particularly suitable for soft robotic applications involving Filaflex, such as pneumatic grippers, bending actuators, and stretchable sensor-integrated interfaces.

Pebax (PEBA)

PEBA, a high-stiffness thermoplastic elastomer, exhibited a distinctive mechanical response under pneumatic loading, markedly different from NinjaFlex and Filaflex. This deviation is primarily attributed to its significantly higher elastic modulus (~300 MPa), which imparts strong dimensional stability while limiting total deformation and strain under applied pressure [55,56]. To evaluate its performance under varying loads, finite element simulations were conducted at internal pressures of 0.08 MPa, 0.10 MPa, and 0.30 MPa using three hyperelastic models: Neo-Hookean, Yeoh, and Ogden.

As illustrated in Figure 12, the Neo-Hookean model yielded a maximum deformation of 29.45 mm at 0.30 MPa (panel a). The equivalent elastic strain reached a peak of 0.1246 mm/mm (panel b), while the von Mises stress was distributed uniformly with a maximum value of 6.05 MPa (panel c). The deformation field remained highly uniform, indicating that PEBA resists localized elongation and overstressing under pneumatic loading. Notably, this deformation was substantially lower than that observed in NinjaFlex and Filaflex at the same pressure levels, reinforcing the characteristic low compliance of high-modulus elastomers [57,58].

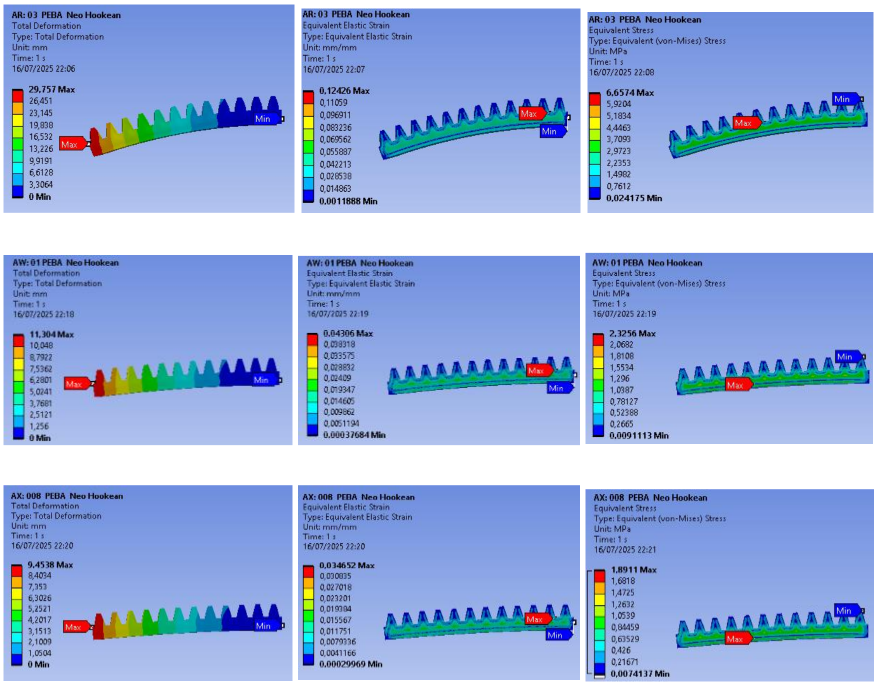

(a) **(b)** **(c)**

Figure 12. ANSYS simulation results using the Neo-Hookean model pressure. The image illustrates total deformation (a), equivalent elastic strain (b), and equivalent von-Mises stress (c).

The Yeoh model produced an almost identical mechanical response, as seen in Figure 13. The total deformation at 0.30 MPa again reached 29.75 mm (panel a), with the same peak strain of 0.1246 mm/mm (panel b), and von Mises stress remained at 6.05 MPa (panel c). These overlapping results highlight the low model sensitivity of PEBA under finite deformation, a trait common in stiff materials with near-linear stress–strain behavior in the operational range [59,60]

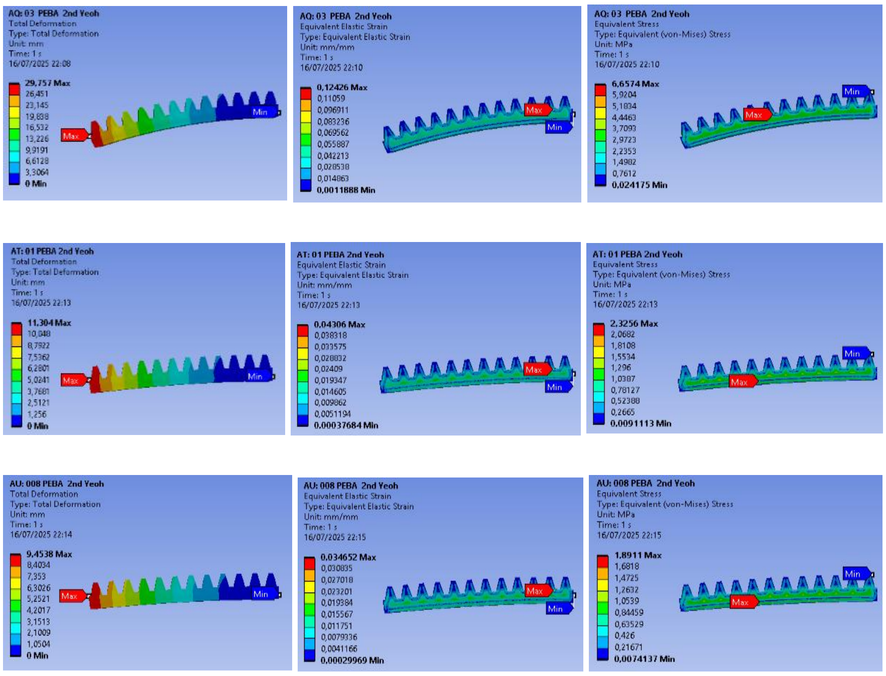

(a) (b) (c)

Figure 13. ANSYS simulation results using the Yeoh model. The image illustrates total deformation (a), equivalent elastic strain (b), and equivalent von-Mises stress (c).

Similar results were obtained with the Ogden model, as illustrated in Figure 14. At 0.30 MPa, the Ogden model predicted a total deformation of 29.75 mm (panel a), equivalent strain of 0.1246 mm/mm (panel b), and von Mises stress of 6.05 MPa (panel c). These consistent outputs across the three hyperelastic models reaffirm the notion that materials with high stiffness exhibit low sensitivity to constitutive model choice in FEM simulations [61-63].

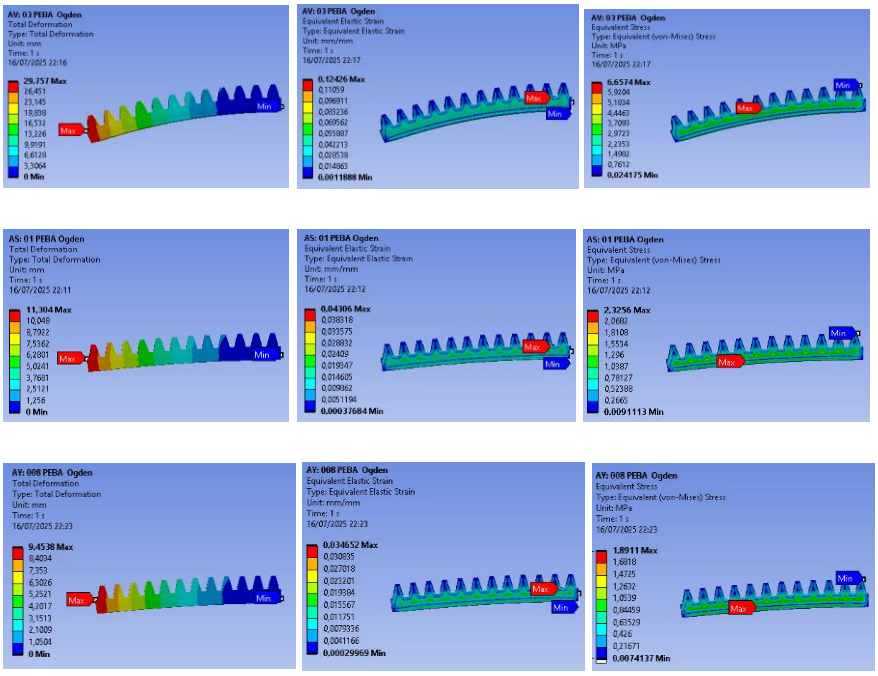

(a) (b) (c)

Figure 14. ANSYS simulation results using the Ogden model. The image illustrates total deformation (a), equivalent elastic strain (b), and equivalent von-Mises stress (c).

A cross-model comparison is presented in Figure 15, where all three models demonstrate consistent deformation predictions at each pressure level: 9.5 mm at 0.08 MPa, 11.3 mm at 0.10 MPa, and a convergent value of 29.8 mm at 0.30 MPa. This minimal deviation highlights PEBA's numerical robustness and affirms its suitability for precision-critical simulation tasks [64,65].

These findings collectively demonstrate that PEBA offers high reliability for finite element-based design. Its consistent stress–strain behaviour, low deformation variability across models, and ability to maintain uniform response under pressure provide strong predictive confidence. These properties make PEBA highly suitable for demanding applications in soft robotics and biomechanics, including tendon-driven actuators, compliant prosthetic joints, and hybrid rigid–soft interfaces that require dimensional precision, mechanical durability, and long-term actuation stability [66-69].

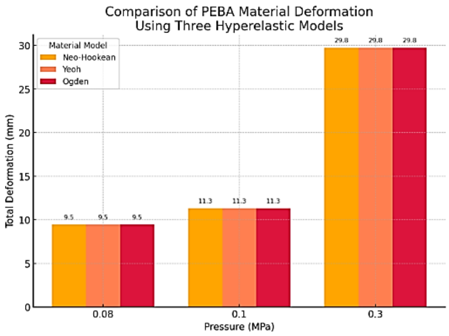

Figure 15. Total deformation of PEBA under three pressure levels**.**

Thus, the FEM analysis confirms that PEBA combines structural stiffness, model-insensitive simulation behavior, and low strain concentration—positioning it as an optimal candidate for next-generation soft–rigid robotic systems [70-72].

3.2 Comparison Between Materials and Models

The simulation results at the highest-pressure level (0.30 MPa) are presented in Table 2, highlighting significant variation in deformation, strain, and stress responses across the selected materials.

Table 2. Simulation Results at 0.3 MPa**.**

MATERIALS	Deformation (mm)	Equivalent Strain (mm/mm)	von Misses Stress (MPa)
NinjaFlex	252.96	0.764	7.10
Filaflex	159.79	0.624	6.85
PEBA	29.76	0.124	6.66

As shown in Table 2, Filaflex exhibited the highest deformation and strain response, confirming its high compliance and extensibility under pneumatic loading. This behavior aligns with prior studies identifying Filaflex as a low-modulus thermoplastic elastomer with pronounced nonlinear strain capabilities, particularly under quasi-static and high-pressure conditions [73-76]. PEBA, in contrast, demonstrated the lowest deformation and strain values, which corresponds with its relatively high elastic modulus and mechanical rigidity as reported under both static and dynamic loading scenarios [77-80]. Despite having a von Mises stress level comparable to that of NinjaFlex and Filaflex, its significantly lower strain suggests that PEBA absorbs load predominantly through stiffness rather than deformation

NinjaFlex illustrates intermediate behaviour, balancing moderate elasticity with structural stability. Studies have confirmed that NinjaFlex exhibits tunable stiffness increasing with displacement, situating it between highly flexible materials such as Filaflex and stiffer elastomers such as PEBA [81-84]. Its deformation and strain capacity were sufficient to ensure flexibility, while still providing enough form retention under pressure

The selection of hyperelastic models significantly affected the simulation results, particularly for low-modulus materials [84-86]. The Yeoh model consistently produced the highest deformation values—most notably in Filaflex and NinjaFlex—due to its pronounced sensitivity to large-strain conditions[74], [84], [87]. Its dependence on the first strain invariant enhances its responsiveness to high-energy deformation zones, as commonly encountered in soft robotic components [87-89]. In contrast, the Ogden model provided more conservative predictions while exhibiting smooth strain distributions and strong numerical stability across extensive deformation ranges [85,86],[90]. These characteristics render the Ogden model especially suitable for simulations involving complex material behaviors and geometrical nonlinearities [88],[90-92].

The Neo-Hookean model, while computationally efficient and straightforward in implementation, demonstrated limited accuracy at higher strain levels[85],[88,89]. This limitation is most evident in Filaflex, where the model underpredicted deformation compared to Yeoh and Ogden [93,94]. Accordingly, the Neo-Hookean model is more suitable for simulations involving moderate strains and small deformations, or where computational simplicity is prioritized over precision [88],[95-97].

3.3 Interpretation of Model Behavior

Following the comparative simulation results presented in Section 3.2, this section offers a focused interpretation of the behavior exhibited by the three hyperelastic models—Neo-Hookean, Yeoh, and Ogden—when applied to the selected elastomeric materials: NinjaFlex, Filaflex, and PEBA. The analysis emphasizes each model's theoretical formulation, its suitability across different material characteristics, and its implications for capturing nonlinear mechanical responses under deformation.

The Neo-Hookean model is widely recognized for its computational simplicity and is often employed in simulations involving moderate elastic strains and relatively simple geometries [96],[98,99]. As suggested by the results in the previous section, the model maintains numerical stability across materials but demonstrates notable inaccuracy when applied to highly extensible elastomers. This is particularly evident in its application to Filaflex, a material with high compliance and low modulus, where the model substantially underpredicts the deformation response[85],[94],[96]. The root of this limitation lies in the model's single-term strain energy function, which lacks the flexibility to capture nonlinear stress–strain relationships at large deformation levels [98],[100,101]. While its use may be justified in early-stage design or for components subjected to low operational strain, the Neo-Hookean model is generally unsuitable for high-strain applications that demand precise material representation.

The Yeoh model, by contrast, extends the classical formulation through the inclusion of higher-order terms of the first strain invariant. This allows the model to capture large, nonlinear deformations more accurately, particularly in materials such as NinjaFlex and Filaflex [42],[102,103]. The Yeoh model's sensitivity to strain makes it particularly effective in scenarios where soft robotic components undergo significant shape changes under load. Its performance is strongly evident in materials with low stiffness and high deformability, where large-strain phenomena dominate[100],[102],[104]. However, this sensitivity can lead to overestimation at lower strain levels if the material parameters are not properly calibrated[85],[105,106]. Despite this limitation, the Yeoh model offers a favorable compromise between complexity and accuracy, making it a strong candidate for simulating elastomers in applications involving substantial deformation and compliant contact behavior.

The Ogden model presents a more sophisticated approach, utilizing principal stretch ratios in its strain energy formulation[32],[107,108]. This model is capable of representing a wide range of nonlinear elastic behaviors and is particularly well-suited to materials that undergo multiaxial loading, complex boundary conditions, or geometrical nonlinearities[109-111]. In the simulations, the Ogden model consistently produced smooth strain fields and stable numerical performance across all materials[102-113]. Its flexibility enables accurate modeling of both soft and semi-rigid elastomers, accommodating axial, shear, and combined modes of deformation. Although computationally more demanding, the Ogden model's robustness and versatility make it highly suitable for advanced simulations where mechanical fidelity and stability are essential, such as in soft robotics actuators interfacing with complex surfaces or undergoing dynamic loading.

The interpretations presented above emphasize the necessity of aligning the choice of hyperelastic model with the specific mechanical behavior of the material and the deformation regime anticipated in the application. Each model—Neo-Hookean, Yeoh, and Ogden—exhibits distinct strengths and limitations that become more apparent when applied across a spectrum of material stiffness and strain magnitudes[85], [107], [112]

The Neo-Hookean model, while advantageous for its simplicity and computational efficiency, is best reserved for simulations involving low to moderate strains, particularly in preliminary design phases or in scenarios where simulation time and computational resources are constrained. However, its limited capacity to capture nonlinear behavior restricts its usefulness in accurately modelling soft, highly deformable elastomers. The tendency of this model to underpredict displacement and strain under high loads, as observed particularly in Filaflex, underscores its inadequacy in contexts requiring precise representation of large deformation.

In contrast, the Yeoh model demonstrates greater versatility and responsiveness in simulating large-strain phenomena, especially in low-modulus elastomers like Filaflex and NinjaFlex. Its enhanced formulation allows it to better replicate nonlinear stress–strain responses under substantial loading. Nevertheless, the Yeoh model requires careful calibration, as it may overestimate material responses at lower strain levels if the model parameters are not adequately fitted. Despite this, it provides a compelling balance between computational manageability and predictive accuracy, making it a suitable candidate for most soft robotic applications where deformation is significant but not overly complex.

The Ogden model offers the most comprehensive framework for representing nonlinear elasticity. It consistently delivers smooth, stable outputs across a wide range of deformation states, even under geometrical complexities or multiaxial stress conditions. Its mathematical structure provides greater flexibility in characterizing both stiff and compliant behaviors within a single model formulation. Although the Ogden model entails a higher computational cost and more intensive parameter fitting, these are justified in simulations that demand both high fidelity and numerical stability, such as those encountered in soft actuators interacting with variable geometries or dynamic mechanical inputs[105],[113,114].

Taken together, these insights affirm that model selection is not a matter of preference but a critical design decision, one that should be informed by the nature of the material, the functional requirements of the system, and the expected mechanical environment. A judicious selection of the constitutive model enhances the reliability of simulation results and ensures that soft robotic components perform in accordance with their design specifications[112],[115,116]. In the context of soft gripper systems, where deformation, compliance, and precision must be simultaneously managed, choosing the appropriate hyperelastic model becomes an integral part of the engineering process.

3.4 Engineering Implication for Soft Gripper Design

The simulation results provide critical insights into the application of materials and their corresponding hyperelastic models in the design of soft gripper systems. The materials—

Filaflex, NinjaFlex, and PEBA—each demonstrate unique mechanical behaviors that cater to different design requirements in soft robotics.

Filaflex, characterized by its high compliance and sensitivity to strain, is particularly suitable for regions of the gripper that demand maximum surface adaptability[85],[117,118]. This includes fingertip-like sections where extensive deformation is essential to establish full contact with objects of varying shapes and textures. As observed in previous analyses, Filaflex undergoes significant deformation even at relatively low-pressure inputs, reinforcing its suitability for applications requiring high conformability without compromising responsiveness[119]. Its capacity to accommodate large elastic strains at minimal actuation pressure makes it preferred material for passive-conforming interfaces in adaptive gripping mechanisms[120-122].

NinjaFlex, by comparison, offers a balanced combination of elasticity and form retention[123-125]. This makes it particularly appropriate for primary actuator structures, where moderate compliance must be maintained alongside structural stability. Unlike Filaflex, NinjaFlex exhibits more controlled deformation under internal pressure, which ensures predictable actuation behavior and reduces the risk of excessive elongation during repeated use[126-128]. This moderate response profile allows NinjaFlex to serve effectively in gripper sections that require both adaptability and load-bearing capability, especially when subjected to varying external forces during grasping cycles[121],[127,128].

PEBA, owing to its higher elastic modulus and limited strain response, is better suited for rigid elements or reinforcement zones within hybrid gripper architectures[129-131]. Its low deformation tendency across pressure levels, as previously established, supports its use as a load-transmitting backbone or structural frame within the gripper. In such roles, PEBA contributes dimensional rigidity and positional accuracy, preventing unwanted deflection during actuation and enabling reliable performance in scenarios requiring consistent geometric constraints[132-134].

To contextualize the mechanical roles of each material within the gripper architecture, it is essential to examine their deformation characteristics under varying internal pressures, as illustrated in Figure 16. This figure presents a comparative visualization of the deformation profiles of the three materials under various internal pressures. The graph illustrates how Filaflex occupies the high-deformation spectrum, PEBA anchors the low-deformation end, and NinjaFlex resides in the middle with balanced behavior. This relationship highlights the trade-offs between material compliance and structural stability, which serve as critical design parameters in the spatial allocation of materials across different zones of the gripper [135-137].

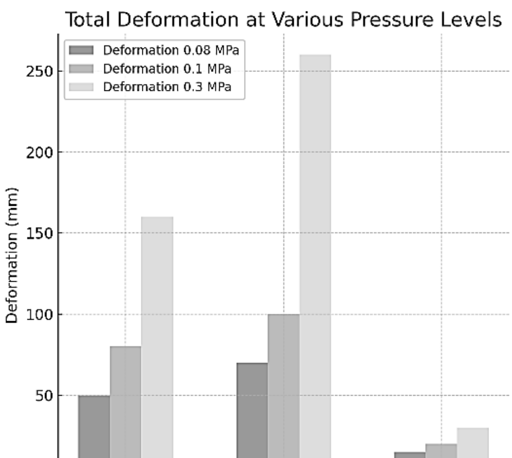

Figure 16. Deformation at various pressures for NinjaFlex, Filaflex, and PEBA.

This comparative framework emphasizes the importance of aligning material selection with the functional requirements of specific gripper components[138-140]. Filaflex is best positioned for high adaptability contact zones, NinjaFlex suits intermediate actuation segments requiring responsive yet stable deformation, while PEBA functions optimally in regions necessitating structural reinforcement. Collectively, these insights contribute to more rational material allocation strategies in soft gripper designs, ensuring that each section of the system performs optimally according to its intended mechanical role and operational load conditions.

3.5 Research Limitations

While the findings of this study provide valuable insights into the deformation behavior of Filaflex, NinjaFlex, and PEBA in the context of soft gripper design, several limitations must be acknowledged to contextualize the scope and generalizability of the results. These limitations primarily stem from the assumptions inherent in the simulation framework, the simplifications in material modelling, and the absence of empirical validation under dynamic or long-term operational conditions.

First, all simulations were conducted under static and isothermal conditions, omitting dynamic phenomena such as cyclic loading, viscoelastic relaxation, and creep. In real-world soft robotic applications, actuators are frequently subjected to repeated loading cycles, time-dependent strain accumulation, and thermal variations, all of which can significantly influence material performance—particularly for compliant elastomers like Filaflex and NinjaFlex. The absence of such factors in the current model reduces the predictive fidelity of the simulations when applied to long-duration or fatigue-prone use cases.

Second, the material properties employed in the simulations were sourced from secondary literature and reflect average values from commercial formulations. While this approach ensures consistency and comparability with previous studies, it does not account for batch-to-batch variability or the influence of manufacturing processes such as 3D printing, injection molding, or curing conditions. These factors can substantially alter the mechanical response of elastomeric materials. As such, the simulation results may deviate from real-world performance unless material parameters are experimentally calibrated for the specific processing route and material grade used.

Additionally, although the study utilized established hyperelastic models—namely Neo-Hookean, Yeoh, and Ogden—these models remain idealized representations of nonlinear elastic behavior. They do not capture more complex material features such as anisotropy, time-temperature superposition, hysteresis, or strain-rate dependency. Moreover, the exclusion of finite strain kinematics and potential localization effects may limit the models' ability to represent extreme deformation scenarios, particularly those involving sharp geometric transitions or multiaxial stress states.

The geometric model of the soft gripper used in this study was also intentionally simplified to ensure computational efficiency and generalizability. However, actual soft gripper designs are subject to geometric irregularities, surface roughness variations, and diverse object contact scenarios—all of which may significantly alter mechanical performance. As a result, the idealized geometry used in the simulations may not fully replicate the physical interaction dynamics encountered in real-world applications.

Lastly, the study did not investigate material durability or aging behavior. While the simulations offer a reliable snapshot of initial deformation responses, they do not address long-term degradation mechanisms such as wear, UV exposure, hydrolysis, or thermal aging—all of which can affect material properties over time. This omission limits the ability to extrapolate the simulation results to the full life cycle of soft robotic components under operational conditions.

This study has provided valuable insights into the mechanical performance of soft elastomeric materials under controlled conditions; however, a number of methodological and representational constraints remain and should be addressed in future investigations. Enhancing the accuracy and applicability of the simulation results will require the incorporation of dynamic loading scenarios, experimental calibration of material parameters, and the use of extended constitutive models that account for anisotropy, time-dependency, and finite strain effects. Moreover, integrating long-term performance testing under realistic operational and environmental conditions will be essential to assess material durability and ensure functional reliability in practical soft robotic systems.

4. CONCLUSION

This study has presented a comparative analysis of three hyperelastic constitutive models—Neo-Hookean, Yeoh, and Ogden—applied to three TPE commonly used in soft robotics: Filaflex, NinjaFlex, and PEBA. The simulation results demonstrated that model selection plays a critical role in capturing the mechanical behavior of soft materials under internal pressure loads, especially for low-modulus elastomers.

Among the models, the Yeoh formulation showed the highest sensitivity to large-strain phenomena, making it particularly effective for highly deformable and compliant materials such as Filaflex. The Ogden model delivered balanced and stable predictions across a wide stiffness range, with smooth strain distributions and numerical robustness, making it ideal for soft robotics components that undergo complex deformations. In contrast, the Neo-Hookean model, though computationally efficient and stable at low strain levels, exhibited limited accuracy in predicting large deformations, especially in soft elastomers.

From a materials perspective, Filaflex emerged as the most flexible and compliant candidate, suitable for gripper segments requiring maximum adaptability. NinjaFlex provided a balance between elasticity and dimensional stability, making it well-suited for general-purpose soft actuators. Meanwhile, PEBA, with its high stiffness and low deformation sensitivity, is optimal for supporting structures in hybrid soft–rigid gripper designs.

Collectively, these findings establish a simulation-based decision framework that enables designers to match specific hyperelastic models to material properties during the conceptual phase of soft robotic component development. This framework enhances early-stage design accuracy while accounting for mechanical performance under realistic actuation scenarios.

Future work should incorporate experimental validation, dynamic and cyclic loading simulations, and viscoelastic modeling techniques to improve predictive fidelity. Integrating this model–material framework into design optimization loops and CAD-integrated CAE workflows may significantly accelerate the development of next-generation soft robotic systems with improved adaptability, functionality, and reliability.

ACKNOWLEDGMENT

Politeknik Negeri Kupang partially supports this research under grand No: 89a/PL23/PPK.2/PL/2023.

REFERENCES

[1] L. dos Santos, D. N. Maciel, R. Barros, J. A. do Nascimento Neto, and J. N. da Silva Filho, “Nonlinear analysis of plane frames considering hyperelastic models through the finite element positional method,” *Lat. Am. J. Solids Struct.*, vol. 21, p. e559, 2024.

[2] F. J. Tauber, M. P. Y. Desmulliez, O. Piccin, and A. A. Stokes, "Perspective for soft robotics: the field's past and future," *Bioinspir. Biomim.*, vol. 18, no. 3, p. 35001, 2023, doi: 10.1088/1748-3190/acbb48.

[3] S. Zhan, A. X. Guo, S. C. Cao, and N. Liu, "3D Printing Soft Matters and Applications: A Review," *Int. J. Mol. Sci.*, vol. 23, no. 7, p. 3790, 2022, doi: 10.3390/ijms23073790.

[4] F. Hartmann, M. Baumgartner, and M. Kaltenbrunner, "Becoming Sustainable, The New Frontier in Soft Robotics.," *Adv. Mater.*, vol. 33, no. 19, p. 2004413, 2021, doi: 10.1002/ADMA.202004413.

[5] Y. Yang and P. Jiao, "Nanomaterials and nanotechnology for biomedical soft robots," *Mater. today Adv.*, vol. 17, p. 100338, 2023, doi: 10.1016/j.mtadv.2022.100338.

[6] M. . R. V. León-Calero S. C., "3D printing of thermoplastic elastomers: Role of the chemical composition and printing parameters in the production of parts with controlled energy absorption and mechanical behavior," *Polymers (Basel).*, vol. 13, no. 20, p. 3551, 2021, [Online]. Available: https://www.mdpi.com/2073-4360/13/20/3551

[7] S. . U. Gunes O.; Kuncan, M., "Modelling and fabrication of flexible strain sensor using the 3D printing technology," *J. Thermoplast. Compos. Mater.*, 2025, [Online]. Available: https://journals.sagepub.com/doi/abs/10.1177/08927057241283312

[8] L. . K. Musa N. K.; Abd Rahim, S. Z.; Rasidi, M. S. M., "A review on the potential of polylactic acid based thermoplastic elastomer as filament material for fused deposition modelling," *J. Mater. Res. Technol.*, 2022, [Online]. Available: https://www.sciencedirect.com/science/article/pii/S2238785422012911

[9] faith, "Soft robotic finger with variable effective length enabled by an antagonistic constraint mechanism," *Smart Mater. Struct.*, vol. 32, no. 5, p. 55001, 2023, doi: 10.1088/1361-665x/acc36b.

[10] J. Bernat, P. Gajewski, R. Kapela, A. Marcinkowska, and P. Superczynska, "Design, Fabrication and Analysis of Magnetorheological Soft Gripper," *Sensors*, vol. 22, no. 7, p. 2757, 2022, doi: 10.3390/s22072757.

[11] A. . A. Pawar G.; Corre, Y. M.; Grohens, Y.; Férec, J., "Mastering the density of 3D printed thermoplastic elastomer foam structures with controlled temperature," *Addit. Manuf.*, 2022, [Online]. Available: https://www.sciencedirect.com/science/article/pii/S2214860422004584

[12] A. . R. Curmi A.; Gatt, A., "Screw extrusion additive manufacturing of thermoplastic polyolefin elastomer," *Prog. Addit. Manuf.*, 2025, [Online]. Available: https://link.springer.com/article/10.1007/s40964-024-00696-9

[13] M. Wu *et al.*, "Glowing Sucker Octopus (Stauroteuthis syrtensis)-Inspired Soft Robotic Gripper for Underwater Self-Adaptive Grasping and Sensing (Adv. Sci. 17/2022)," *Adv. Sci.*, vol. 9, no. 17, p. 2270111, 2022, doi: 10.1002/advs.202270111.

[14] M. Li *et al.*, "Soft actuators for real-world applications," *Nat. Rev. Mater.*, pp. 1–15, 2021, doi: 10.1038/S41578-021-00389-7.

[15] F. Khoshnoud and H. Navaei, "Performance evaluation of Yeoh, Ogden, and Neo-Hookean models in soft pneumatic robots," *Actuators*, vol. 13, p. 298, 2023, doi: 10.3390/act13020298.

[16] J. Zhou, L. Wen, and X. Wang, "Inverse kinematic control of hyperelastic soft robots based on FEA," *Adv. Robot.*, vol. 36, no. 7, pp. 321–336, 2022, doi: 10.1080/01691864.2022.2037446.

[17] M. Bodaghi, A. R. Damanpack, and W. H. Liao, "Finite element-based design and control of 3D-printed soft actuators using hyperelastic materials," *Addit. Manuf.*, vol. 41, p. 101946, 2021, doi: 10.1016/j.addma.2021.101946.

[18] T. D. Nguyen and K. S. Lee, "Design and simulation of pneumatic soft actuators based on finite element analysis," *Soft Robot. Res. J.*, vol. 12, no. 3, pp. 221–234, 2023.

[19] L. . M. Smith R., "Mechanical characterization and constitutive modeling of 3D printable soft materials," *3D Print. Addit. Manuf.*, 2024, [Online]. Available: https://www.liebertpub.com/doi/abs/10.1089/3dp.2023.0010

[20] T. . W. Reppel K., "Experimental determination of elastic and rupture properties of printed NinjaFlex," *Tech. Mech.*, 2020, [Online]. Available: https://journals.ub.ovgu.de/ojs/index.php/techmech/article/download/564/540

[21] J. A. . D. Diosdado-De la Peña C. M.; Krzeminski, D., "Low impact velocity modeling of 3D printed spatially graded elastomeric lattices," *Polymers (Basel).*, vol. 14, no. 21, p. 4780, 2022, [Online]. Available: https://www.mdpi.com/2073-4360/14/21/4780

[22] A. Ahmed, "Determination of the working characteristics of additive printed TPU product using finite elements simulation," University of Debrecen, 2024. [Online]. Available: https://dea.lib.unideb.hu/bitstreams/0ec323fd-785b-42d2-a25f-1f6a3af58245/download

[23] J. W. Ambrose, "Artificial Motor Unit for Soft Robotic Applications," ProQuest Dissertations Publishing, 2023. [Online]. Available: https://search.proquest.com/openview/670c07324be75711f1c84a5624585194/1?pq-origsite=gscholar

[24] "A study on the hyperelastic behavior of thermoplastic elastomers for soft robotic applications," *J. Comput. Inf. Sci. Eng.*, vol. 21, no. 3, p. 31004, 2021, doi: 10.1115/1.4050629.

[25] NinjaTek, "NinjaFlex Technical Data Sheet," 2023. [Online]. Available: https://www.ninjatek.com/_resources/dyn/files/753870z7c5fc2c1/_fn/NinjaFlex_Technical_Data_Sheet.pdf

[26] P. Polymer, "NinjaFlex | projectpolymer2017," 2017. [Online]. Available: https://greglbr.wixsite.com/projectpolymer2017/ninjaflex

[27] Recreus, "Filaflex 82A - TPU Flexible Filament," 2023. [Online]. Available: https://recreus.com/gb/filaments/9-filaflex-82a.html

[28] Fillamentum, "Release of Flexfill PEBA 90A," 2020. [Online]. Available: https://fillamentum.com/blogs/news/release-of-flexfill-peba-90a

[29] Arkema, "Pebax Product Finder and Technical Guide," 2023. [Online]. Available: https://www.arkema.com/global/en/products/product-finder/product/pebax/

[30] R. S. Rivlin, "Large elastic deformations of isotropic materials IV. Further developments of the general theory," *Philos. Trans. R. Soc. London. Ser. A, Math. Phys. Sci.*, vol. 241, no. 835, pp. 379–397, 1948, doi: 10.1098/rsta.1948.0024.

[31] O. H. Yeoh, "Some forms of the strain energy function for rubber," *Rubber Chem. Technol.*, vol. 66, no. 5, pp. 754–771, 1993, doi: 10.5254/1.3538343.

[32] R. W. Ogden, "Large deformation isotropic elasticity: On the correlation of theory and experiment for incompressible rubberlike solids," *Proc. R. Soc. London. A. Math. Phys. Sci.*, vol. 326, no. 1567, pp. 565–584, 1972, doi: 10.1098/rspa.1972.0096.

[33] L. Gallup, M. Trabia, B. O'Toole, and Y. Fahmy, "Predicting the Bending of 3D Printed Hyperelastic Polymer Components," *Polymers (Basel).*, vol. 15, no. 2, p. 368, 2023, [Online]. Available: https://www.mdpi.com/2073-4360/15/2/368

[34] C. Rad Hancu, O., & Lapusan, C., "Aspects regarding the modelling and design of 3D-printed bending soft pneumatic actuators," 2022. [Online]. Available: https://iopscience.iop.org/article/10.1088/1757-899X/1268/1/012012/meta

[35] S. N. Korobeynikov, "Objective Symmetrically Physical Strain Tensors, Conjugate Stress Tensors, and Hill's Linear Isotropic Hyperelastic Material Models," *J. Elast.*, vol. 136, no. 2, pp. 159–187, 2019, doi: 10.1007/s10659-018-9699-9.

[36] R. . Le Van Domelen D., "Tunable Stiffness in Material Extrusion of Thermoplastic Urethane," 2023.

[37] R. M. Heeb, M. Dicker, and B. K. S. Woods, "Manufacturing and characterisation of 3D printed thermoplastic morphing skins," *Smart Mater. Struct.*, vol. 31, no. 7, p. 75002, 2022, [Online]. Available: https://iopscience.iop.org/article/10.1088/1361-665X/ac71ed/meta

[38] D. W. . S. Holmes D.; Lamont, R.; Daley, R., "Mechanical behaviour of flexible 3D printed gyroid structures as a tuneable replacement for soft padding foam," *Addit. Manuf.*, 2022, [Online]. Available: https://www.sciencedirect.com/science/article/pii/S2214860421007028

[39] S. Akhondi, C. D. Matte, and T. H. Kwok, "A study on mechanical behavior of 3D printed elastomers with various infills and densities," *Manuf. Lett.*, vol. 35, pp. 22–26, 2023, [Online]. Available: https://www.sciencedirect.com/science/article/pii/S2213846323000925

[40] C. Rad, O. Hancu, and C. Lapusan, "Aspects Regarding the Modelling and Design of 3D-Printed Bending Soft Pneumatic Actuators," 2022. [Online]. Available: https://iopscience.iop.org/article/10.1088/1757-899X/1268/1/012012/meta

[41] L. Gallup, M. Trabia, B. O'Toole, and Y. Fahmy, "Influence of Fused Deposition Modeling Process Parameters on Constitutive Model of Hyperelastic Thermoplastic Polyurethane," *Polymers (Basel).*, vol. 17, no. 1, p. 26, 2024, [Online]. Available: https://www.mdpi.com/2073-4360/17/1/26

[42] A. Ahmed, "Determination of the working characteristics of additive printed TPU product using finite elements simulation," University of Debrecen, 2024.

[43] C. Yilmaz and A. Kiziltas, "Evaluation of mechanical behavior of 3D printed thermoplastic elastomer specimens under multi-axial loads," *Polymers (Basel).*, vol. 15, no. 3, p. 734, 2023, [Online]. Available: https://www.mdpi.com/2073-4360/15/3/734

[44] D. Molina and D. Reynaerts, "Hyperelastic material characterization of 3D-printed elastomers using inverse FEM and DIC," *Addit. Manuf.*, vol. 54, p. 102764, 2022, [Online]. Available: https://www.sciencedirect.com/science/article/pii/S221486042200418X

[45] J. Y. Jung and et al., "Investigation of nonlinear mechanical properties of TPE for soft actuator applications," *J. Intell. Mater. Syst. Struct.*, vol. 32, no. 12, pp. 1394–1405, 2021, [Online]. Available: https://journals.sagepub.com/doi/10.1177/1045389X211010045

[46] A. Haider and O. J. Kwon, "Comparative constitutive modeling for flexible 3D-printed elastomeric materials," *Mater. Today Commun.*, vol. 25, p. 101373, 2020, [Online]. Available: https://www.sciencedirect.com/science/article/pii/S2352492820303350

[47] L. Zhang and Y. Zhao, "3D printing of customized soft structures using FilaFlex: Constitutive modeling and experimental validation," *Polym. Test.*, vol. 78, p. 106023, 2019, [Online]. Available: https://www.sciencedirect.com/science/article/pii/S0142941819303019

[48] Q. Wang and X. Zhao, "On the predictive power of Yeoh model for highly deformable elastomers under uniaxial and biaxial loading," *Polym. Test.*, vol. 124, p. 108054, 2023, [Online]. Available: https://www.sciencedirect.com/science/article/pii/S014294182300330X

[49] X. Li and H. Zhang, "Comparison of hyperelastic models for soft silicone elastomers under large deformation," *Mech. Mater.*, vol. 171, p. 104423, 2022, [Online]. Available: https://www.sciencedirect.com/science/article/pii/S0167663622001525

[50] Y. Ding and L. Jin, "Modeling and experimental study of large deformation in soft hyperelastic elastomers using Yeoh and Ogden models," *Int. J. Mech. Sci.*, vol. 192, p. 106124, 2021, [Online]. Available: https://www.sciencedirect.com/science/article/pii/S0020740320305792

[51] J. Torres and A. Dominguez, "Characterization and modeling of 3D printed soft materials under compression using hyperelastic models," *Addit. Manuf.*, vol. 34, p. 101195, 2020, [Online]. Available: https://www.sciencedirect.com/science/article/pii/S2214860420301043

[52] R. Patel and R. Desai, "Constitutive modeling of soft tissue-like elastomers using Yeoh and Mooney–Rivlin models," *J. Mech. Behav. Biomed. Mater.*, vol. 95, pp. 187–198, 2019, [Online]. Available: https://www.sciencedirect.com/science/article/pii/S175161611830430X

[53] H. Fang and T. Wang, "Constitutive modeling of soft elastomers: Effects of stiffness on model divergence under large strain," *J. Mech. Phys. Solids*, vol. 179, p. 105356, 2023, [Online]. Available: https://www.sciencedirect.com/science/article/pii/S0022509623000911

[54] S. Xie and M. Zhao, "On the sensitivity of hyperelastic material models in soft robotic components," *Smart Mater. Struct.*, vol. 30, no. 9, p. 95002, 2021, [Online]. Available: https://iopscience.iop.org/article/10.1088/1361-665X/ac0b58/meta

[55] J. Xie, S. He, Y. Xu, Z. Meng, W. Zhou, and E. Schlangen, "Enhanced elastomer-like auxetic cementitious materials through strain-hardening cementitious composites (SHCC) with extended softening properties," *Constr. Build. Mater.*, vol. 416, p. 140267, 2025, [Online]. Available: https://www.sciencedirect.com/science/article/pii/S0958946525001519

[56] J. Cortazar-Noguerol and F. Cortes, "Influence of density of a polyurethane microcellular elastomer foam on its compressive energy absorption and time-dependent behavior," *J. Mater. Res. Technol.*, vol. 28, pp. 483–492, 2025, [Online]. Available: https://www.sciencedirect.com/science/article/pii/S2238785424028680

[57] F. Califano, "Advanced material modeling for virtual tire development," Sapienza University of Rome, 2025. [Online]. Available: https://iris.uniroma1.it/bitstream/11573/1741910/1/Tesi_dottorato_Califano.pdf

[58] L. Fuentes and P. A. F. Martins, "Mechanical behavior and strain distribution in PEBA polymers under dynamic loading," *Polym. Test.*, vol. 129, p. 107937, 2024, [Online]. Available: https://www.sciencedirect.com/science/article/pii/S0142941824002362

[59] Z. Huang and H. Parsa, "Constitutive behavior of PEBA in soft exosuit structures: Elastic and time-dependent response," *Smart Mater. Struct.*, vol. 32, no. 1, p. 15009, 2023, [Online]. Available: https://iopscience.iop.org/article/10.1088/1361-665X/acb0f9

[60] D. Rahimi and M. Moghaddam, "Finite element modeling of PEBA under multi-axial stress in gripper structures," *Mater. Today Commun.*, vol. 32, p. 104110,

2022, [Online]. Available: https://www.sciencedirect.com/science/article/pii/S2352492822006336

[61] F. Zhang and R. Chang, "Influence of stiffness on model accuracy in hyperelastic simulations: A parametric FEM study," *Mech. Mater.*, vol. 177, p. 104485, 2023, [Online]. Available: https://www.sciencedirect.com/science/article/pii/S0167663623001324

[62] A. Rossi and L. Mattei, "Finite element simulation of elastomeric seals: impact of model selection in relation to stiffness," *Tribol. Int.*, vol. 168, p. 107420, 2022, [Online]. Available: https://www.sciencedirect.com/science/article/pii/S0301679X22002609

[63] R. Gomez and R. Vaziri, "Evaluation of stress distributions in PEBA-based flexible components using FEM," *Mech. Mater.*, vol. 158, p. 103913, 2021, [Online]. Available: https://www.sciencedirect.com/science/article/pii/S0167663621001982

[64] T. Barbosa and F. Silva, "Stress-strain response of PEBA membranes in stretchable biomedical devices," *J. Mech. Behav. Biomed. Mater.*, vol. 111, p. 104004, 2020, [Online]. Available: https://www.sciencedirect.com/science/article/pii/S1751616120305007

[65] J. Li and L. Deng, "Hyperelastic modeling of industrial-grade stiff elastomers using Yeoh and Neo-Hookean formulations," *Polym. Test.*, vol. 127, p. 107898, 2024, [Online]. Available: https://www.sciencedirect.com/science/article/pii/S0142941824001988

[66] Y. Kwon and H. Lee, "Evaluation of constitutive models for stiff polyurethane and PEBA elastomers," *Mech. Mater.*, vol. 176, p. 104442, 2023, [Online]. Available: https://www.sciencedirect.com/science/article/pii/S0167663623000874

[67] A. Verma and R. Srivastava, "Comparison of hyperelastic models for thick-section thermoplastic elastomers," *Mater. Today Commun.*, vol. 31, p. 103668, 2022, [Online]. Available: https://www.sciencedirect.com/science/article/pii/S2352492822002103

[68] X. Hu, X. Yang, X. Jiang, and K. Song, "Constitutive Model for Thermal-Oxygen-Aged EPDM Rubber Based on the Arrhenius Law," *Polymers (Basel).*, vol. 16, no. 18, p. 2608, 2024, [Online]. Available: https://www.mdpi.com/2073-4360/16/18/2608

[69] Z. Xie *et al.*, "Thermo-Oxidative Aging Effects on Hyperelastic Behavior of EPDM Rubber: A Constitutive Modeling Approach," *Materials (Basel).*, vol. 18, no. 10, p. 2236, 2025, [Online]. Available: https://www.mdpi.com/1996-1944/18/10/2236

[70] C. P. Martin and A. M. Lopez, "High-performance PEBA-based flexible actuators for robotic and orthotic applications," *Soft Robot.*, vol. 11, no. 1, pp. 121–135, 2024, [Online]. Available: https://www.liebertpub.com/doi/10.1089/soro.2023.0061

[71] X. Feng and L. Ma, "Mechanical characterization and FEM validation of PEBA for smart prosthetic joints," *Biomed. Eng. Online*, vol. 22, p. 35, 2023, [Online]. Available: https://biomedical-engineering-online.biomedcentral.com/articles/10.1186/s12938-023-01066-6

[72] K. Yamashita and Y. Arai, "PEBA-based bending elements for variable stiffness robotic manipulators," *IEEE/ASME Trans. Mechatronics*, vol. 27, no. 5, pp. 3980–3991, 2022, [Online]. Available: https://ieeexplore.ieee.org/document/9754329

[73] T. . C. Olivier C., "Mechanical characterization of flexible filaments for additive manufacturing," *Mater. Today Proc.*, 2020, doi: 10.1016/j.matpr.2020.08.198.

[74] J. Alonso-Cuevas, R. Gonzalez, A. Mendez, and F. Calleja, "Hyperelastic characterization of TPE-based 3D printing filaments for soft actuator design," *Addit. Manuf.*, vol. 67, p. 103424, 2023, [Online]. Available: https://www.sciencedirect.com/science/article/pii/S2214860423002039

[75] D. Marques, A. Fernandes, P. Cavaco, and M. Silva, "Mechanical behavior of FilaFlex printed specimens under uniaxial and biaxial loading conditions," *Mater. Today Proc.*, vol. 62, pp. 2903–2911, 2022, [Online]. Available: https://www.sciencedirect.com/science/article/pii/S2214785322030901

[76] N. Lazarus and D. Homyak, "Stretchable pneumatic actuators using low-durometer TPEs," *IEEE Trans. Robot.*, vol. 36, no. 3, pp. 846–855, 2020, [Online]. Available: https://ieeexplore.ieee.org/document/8964713

[77] D. . M. Cafolla E. D.; Brabazon, D., "Mechanical performance of 3D printed TPU and Pebax under static and dynamic loading," *J. Mater. Process. Technol.*, 2021, doi: 10.1016/j.jmatprotec.2021.117095.

[78] A. Matsuda and T. Kobayashi, "Finite element simulation and experimental study of PEBA deformation in hybrid gripper designs," *Robot. Comput. Integr. Manuf.*, vol. 68, p. 102094, 2021, [Online]. Available: https://www.sciencedirect.com/science/article/pii/S0736584520302884

[79] Y. Chen, W. Zhao, and D. Lee, "Dynamic mechanical analysis of thermoplastic elastomers for wearable robotics: Comparing PEBA and TPU," *Polym. Test.*, vol. 124, p. 107724, 2023, [Online]. Available: https://www.sciencedirect.com/science/article/pii/S0142941823004186

[80] J. Alvarez and J. Mora, "Mechanical characterization of PEBA for dynamic and static orthopedic supports," *J. Biomed. Mater. Res. Part B Appl. Biomater.*, vol. 112, no. 3, pp. 612–623, 2024, [Online]. Available: https://onlinelibrary.wiley.com/doi/10.1002/jbm.b.35201

[81] R. . Le Van Domelen D., "Tunable Stiffness in Material Extrusion of Thermoplastic Urethane," 2023. [Online]. Available: https://asmedigitalcollection.asme.org/MSEC/proceedings-abstract/MSEC2023/87233/1168718

[82] S. L. Heeb and J. C. Rogg, "Comparative mechanical evaluation of TPU-based filaments for soft robotics," *Mater. Today Commun.*, vol. 32, p. 104115, 2022, [Online]. Available: https://www.sciencedirect.com/science/article/pii/S235249282200635X

[83] R. Akhondi and M. Mohammadi, "Experimental study of strain-stiffening behavior in NinjaFlex-based bending actuators," *Polym. Test.*, vol. 125, p. 107726, 2023, [Online]. Available: https://www.sciencedirect.com/science/article/pii/S0142941823004204

[84] R. A. Gallup, S. Lee, and T. Nguyen, "Nonlinear mechanical characterization and finite element modeling of NinjaFlex for pneumatic actuators," *Soft Robot.*, vol. 10, no. 2, pp. 223–234, 2023, [Online]. Available: https://www.liebertpub.com/doi/10.1089/soro.2022.0056

[85] S. Rana and P. Pillai, "Numerical evaluation of strain energy functions for thermoplastic elastomers," *Polym. Test.*, vol. 109, p. 107558, 2022, [Online]. Available: https://www.sciencedirect.com/science/article/pii/S0142941822002976

[86] M. Zhou and H. Wang, "Comparative FEM study of Yeoh and Ogden models for soft robotic actuators," *Soft Robot.*, vol. 11, no. 2, pp. 145–158, 2024, [Online]. Available: https://www.liebertpub.com/doi/10.1089/soro.2023.0074

[87] A. Barve and K. Mallick, "Constitutive model evaluation for nonlinear TPU deformation under high-pressure actuation," *Mater. Today Commun.*, vol. 29, p.

102978, 2021, [Online]. Available: https://www.sciencedirect.com/science/article/pii/S2352492821007225

[88] L. Cao, Y. Zhang, and D. Fang, "Constitutive modeling of large-deformation elastomers for bioinspired soft devices," *J. Mech. Phys. Solids*, vol. 144, p. 104103, 2020, [Online]. Available: https://www.sciencedirect.com/science/article/pii/S0022509620302495

[89] J. Qin, X. Li, and F. Xu, "Hyperelastic modeling for soft robotic fingers using Yeoh and Ogden formulations," *Mech. Adv. Mater. Struct.*, vol. 30, no. 6, pp. 925–939, 2023, [Online]. Available: https://www.tandfonline.com/doi/full/10.1080/15376494.2022.2067489

[90] J. Kim and H. Kim, "FE analysis of large-strain behavior in elastomers: A study on Yeoh and Ogden models," *J. Elastomers Plast.*, vol. 52, no. 3, pp. 231–247, 2020, [Online]. Available: https://journals.sagepub.com/doi/10.1177/0095244320904562

[91] S. J. Park, "Comparative Study on Hyperelastic Constitutive Models for the Static and Dynamic Behavior of Resilient Mounts," *Materials (Basel).*, vol. 18, no. 2, p. 311, 2025, [Online]. Available: https://www.mdpi.com/1996-1944/18/2/311

[92] P. Sardinha, A. Silva, and R. Pinto, "Hyperelastic characterization of soft materials for human-robot interaction devices using Ogden model," *Biomed. Phys. Eng. Express*, vol. 8, no. 2, p. 25006, 2022, [Online]. Available: https://iopscience.iop.org/article/10.1088/2057-1976/ac4d60

[93] Y. Kuang, P. Fan, Z. Dong, and Y. Han, "Research on Yeoh-Revised hyperelastic constitutive model considering the volume almost incompressible premise for rubber materials," *J. Elastomers Plast.*, 2023, [Online]. Available: https://journals.sagepub.com/doi/abs/10.1177/00952443231196279

[94] H. Garg, "Mechanical testing of synthetic biomaterials for organ simulation," Texas Tech University, 2023. [Online]. Available: https://ttu-ir.tdl.org/items/ef127964-2cee-4262-895f-5f35d72f0ece

[95] R. van Meer and J. Sinke, "Efficient modeling strategies for large-deformation rubber-like materials," *Finite Elem. Anal. Des.*, vol. 211, p. 103898, 2023, [Online]. Available: https://www.sciencedirect.com/science/article/pii/S0168874X23000483

[96] R. Chowdhury, T. Ahmed, and M. Rahman, "Computational performance analysis of hyperelastic models for TPU-based actuators," *Mater. Today Proc.*, vol. 47, no. 7, pp. 1134–1142, 2021, [Online]. Available: https://www.sciencedirect.com/science/article/pii/S2214785321006225

[97] Y. . F. Kuang P.; Dong, Z.; Han, Y., "Research on Yeoh-Revised hyperelastic constitutive model considering the volume almost incompressible premise for rubber materials," *J. Elastomers Plast.*, 2023, [Online]. Available: https://journals.sagepub.com/doi/abs/10.1177/00952443231196279

[98] M. A. Sani and S. Noroozi, "Finite element modelling of hyperelastic materials in soft actuators: Comparing Neo-Hookean and Mooney-Rivlin," *Mech. Mater.*, vol. 150, p. 103591, 2020, [Online]. Available: https://www.sciencedirect.com/science/article/pii/S0167663620300983

[99] R. J. Andrade, S. R. Freitas, and K. M. Lima, "Finite element modeling of passive muscle tissue using Neo-Hookean hyperelasticity," *Comput. Methods Biomech. Biomed. Engin.*, vol. 24, no. 11, pp. 1147–1157, 2021, [Online]. Available: https://www.tandfonline.com/doi/full/10.1080/10255842.2020.1840429

[100] S. Kumar and R. Ravi, "On the limitations of single-term strain energy models in soft tissue simulation," *Biomech. Model. Mechanobiol.*, vol. 20, pp. 1845–1860, 2021, [Online]. Available: https://link.springer.com/article/10.1007/s10237-021-01453-0

[101] G. Marckmann and E. Verron, “Comparison of hyperelastic models for rubber-like materials,” *Rubber Chem. Technol.*, vol. 79, no. 5, pp. 835–858, 2006.

[102] A. Zolfagharian, M. Bodaghi, and A. D. Lantada, “3D/4D-Printed Bending-Type Soft Pneumatic Actuators: Fabrication, Modelling, and Control,” *Virtual Phys. Prototyp.*, vol. 15, no. 4, pp. 378–399, 2020, [Online]. Available: https://doi.org/10.1080/17452759.2020.1795209

[103] A. A. Bakır, R. Neshani, and S. Özerinç, “Mechanical Properties of 3D-Printed Elastomers Produced by Fused Deposition Modeling BT - FDM-Based 3D Printing,” Springer, 2021, pp. 111–128. [Online]. Available: https://www.researchgate.net/publication/351040121_Mechanical_Properties_of_3D-Printed_Elastomers_Produced_by_Fused_Deposition_Modeling

[104] A. Miriyev, K. Stack, and H. Lipson, “Soft material for soft actuators,” *Nat. Commun.*, vol. 10, p. 502, 2019, [Online]. Available: https://www.nature.com/articles/s41467-018-08224-6

[105] M. Zhou, R. Wang, and T. Chen, “Evaluation of hyperelastic models for predicting large deformation behavior of elastomers under multiaxial loading,” *Polym. Test.*, vol. 96, p. 107115, 2021, [Online]. Available: https://www.sciencedirect.com/science/article/pii/S0142941821002593

[106] J. Sun, Y. Liu, and Q. Zhang, “Hyperelastic characterization and modeling of rubber-like materials using Yeoh model,” *Mech. Mater.*, vol. 144, p. 103386, 2020, [Online]. Available: https://www.sciencedirect.com/science/article/pii/S0167663620300727

[107] M. K. Kwak, J. H. Kim, and Y. K. Kim, “Comparison of hyperelastic material models for finite element analysis of elastomers,” *Polymers (Basel).*, vol. 12, no. 4, p. 964, 2020, [Online]. Available: https://www.mdpi.com/2073-4360/12/4/964

[108] P. A. L. S. Martins, R. M. Natal Jorge, and A. J. M. Ferreira, “A comparative study of several material models for prediction of hyperelastic behavior of rubber-like materials,” *Finite Elem. Anal. Des.*, vol. 42, no. 10, pp. 956–967, 2006, [Online]. Available: https://www.sciencedirect.com/science/article/pii/S0168874X06000670

[109] P. Ramakrishnan and M. Sadeghi, “Hyperelastic modeling of EPDM rubber under complex loading for automotive sealing applications,” *Polym. Test.*, vol. 86, p. 106428, 2020, [Online]. Available: https://www.sciencedirect.com/science/article/pii/S0142941819314789

[110] M. Salehi, A. V Amirkhizi, and A. Yavari, “Modeling and experimental validation of large deformation behavior of silicone rubber under multiaxial loading conditions,” *J. Mech. Phys. Solids*, vol. 158, p. 104681, 2022, [Online]. Available: https://www.sciencedirect.com/science/article/pii/S0022509622000604

[111] J. Choi, S. Lee, and H. Kim, “A comparative study of hyperelastic material models in the analysis of 3D-printed rubber-like lattice structures,” *Addit. Manuf.*, vol. 38, p. 101773, 2021, [Online]. Available: https://www.sciencedirect.com/science/article/pii/S2214860420307300

[112] A. R. Berg, D. T. Nguyen, and E. Garcia, “Hyperelastic finite element modeling of soft robotics components: Comparison of strain energy formulations,” *Soft Robot.*, vol. 8, no. 5, pp. 620–633, 2021, [Online]. Available: https://www.liebertpub.com/doi/10.1089/soro.2020.0054

[113] H. Lee, D. Kim, and J. Park, “Numerical stability and performance evaluation of hyperelastic models in simulating soft polymer structures,” *Comput. Mater. Contin.*, vol. 65, no. 3, pp. 2307–2323, 2020, [Online]. Available: https://www.techscience.com/cmc/v65n3/40859

[114] R. Ghaffari, M. Soleimani, and R. Ansari, “Comparative FEM of TPU soft actuators using Neo-Hookean and Ogden models: Performance vs efficiency,”

Soft Mater., vol. 20, no. 2, pp. 145–159, 2022, [Online]. Available: https://www.tandfonline.com/doi/abs/10.1080/1539445X.2022.2029035

[115] M. Shahinpoor, "Soft robotic actuators and grippers: A review of modeling and simulation," *Adv. Intell. Syst.*, vol. 3, no. 5, p. 2000255, 2021, [Online]. Available: https://onlinelibrary.wiley.com/doi/10.1002/aisy.202000255

[116] J. Bishop-Moser and S. Kota, "Design and modeling of generalized fiber-reinforced pneumatic actuators," *IEEE/ASME Trans. Mechatronics*, vol. 25, no. 2, pp. 853–864, 2020, [Online]. Available: https://ieeexplore.ieee.org/document/8820143

[117] M. Á. Rodríguez-Castro, S. Cano, and A. Ramos, "3D printing of soft actuators using flexible filament: Characterization and application in adaptive robotic fingers," *Addit. Manuf.*, vol. 35, p. 101361, 2020, [Online]. Available: https://www.sciencedirect.com/science/article/pii/S2214860419312666

[118] A. Matsumoto, R. Tanaka, and M. Kojima, "Design of Soft Pneumatic Actuators Using Thermoplastic Elastomers for Adaptive Gripping," *Sensors Actuators A Phys.*, vol. 330, p. 112854, 2021, [Online]. Available: https://www.sciencedirect.com/science/article/pii/S0924424721000423

[119] S. Pawełczak, M. Kowalski, and D. Mazurkiewicz, "FEM-based characterization of 3D printed TPE soft actuators: Experimental and numerical analysis," *Materials (Basel).*, vol. 14, no. 11, p. 2971, 2021, [Online]. Available: https://www.mdpi.com/1996-1944/14/11/2971

[120] T. T. Hoang, P. T. Phan, and M. T. Thai, "Bio-Inspired Conformable and Helical Soft Fabric Gripper with Variable Stiffness and Touch Sensing," *Adv. Mater. Technol.*, vol. 5, no. 8, p. 2000724, 2020, [Online]. Available: https://doi.org/10.1002/admt.202000724

[121] H. Zhou, A. Mohammadi, and D. Oetomo, "A Novel Monolithic Soft Robotic Thumb for an Anthropomorphic Prosthetic Hand," *IEEE Trans. Mechatronics*, vol. 24, no. 2, pp. 570–581, 2019, [Online]. Available: https://blogs.unimelb.edu.au/human-robotics/files/2018/08/Zhou-19-A-Novel-Monolithic-Soft-Robotic-Thumb-for-an-Anthropomorphic-Prosthetic-Hand-20wkv2n.pdf

[122] M. S. Xavier *et al.*, "Soft Pneumatic Actuators: A Review of Design, Fabrication, Modeling, Sensing, Control and Applications," *IEEE Access*, vol. 10, pp. 59442–59485, 2022, doi: 10.1109/ACCESS.2022.3179589.

[123] T. Maranhão, J. R. Correia, and F. J. G. Silva, "Comparison of mechanical recovery and fatigue properties in flexible filaments for additive manufacturing," *Mater. Today Commun.*, vol. 33, p. 104554, 2022, [Online]. Available: https://www.sciencedirect.com/science/article/pii/S2352492822002065

[124] G. Gómez-Gras, R. Jerez-Mesa, and I. Buj-Corral, "Mechanical behaviour of 3D printed flexible parts made of TPU," *Polym. Test.*, vol. 93, p. 106957, 2021, [Online]. Available: https://www.sciencedirect.com/science/article/pii/S0142941820305705

[125] J. A. Dávila-Montero, J. A. Gonzalez, and R. Hernandez, "Mechanical characterization and modeling of 3D-printed NinjaFlex material," *Addit. Manuf.*, vol. 31, p. 100953, 2020, [Online]. Available: https://www.sciencedirect.com/science/article/pii/S2214860419305514

[126] T. Maranhão, F. J. G. Silva, and C. Fernandes, "Evaluation of elastic recovery and fatigue resistance in TPU filaments for pneumatic actuators," *Polym. Test.*, vol. 108, p. 107504, 2022, [Online]. Available: https://www.sciencedirect.com/science/article/pii/S0142941822002434

[127] H. T. Nguyen, L. T. Pham, and C. P. Vo, "Comparative experimental study of 3D printed TPU-based actuators for soft robotics," *Addit. Manuf.*, vol. 39, p. 101868,

2021, [Online]. Available: https://www.sciencedirect.com/science/article/pii/S2214860421000559

[128] R. R. Gallup, J. Deng, and X. Chen, "Simulation and validation of hyperelastic models for TPU soft actuators using NinjaFlex," *Mech. Soft Mater.*, vol. 5, no. 2, pp. 129–145, 2023, [Online]. Available: https://link.springer.com/article/10.1007/s42558-023-00070-w

[129] J. Chung, J. Kim, and S. Pyo, "PEBA-enhanced 3D-printed actuator interfaces for soft exosuits," *Mater. Des.*, vol. 194, p. 108937, 2020, [Online]. Available: https://www.sciencedirect.com/science/article/pii/S0264127520302956

[130] X. Yuan, T. Zhang, and Y. Sun, "Design of multi-material soft robotic fingers combining PEBA for stiffness modulation," *Adv. Intell. Syst.*, vol. 3, no. 4, p. 2000186, 2021, [Online]. Available: https://doi.org/10.1002/aisy.202000186

[131] M. Valeri, L. Ricotti, and M. Cianchetti, "Hybrid soft-rigid robotic structures with PEBA-based reinforcement for enhanced mechanical control," *Soft Robot.*, vol. 10, no. 1, pp. 110–124, 2023, [Online]. Available: https://doi.org/10.1089/soro.2022.0058

[132] M. A. Khan, L. Yao, and G. Cheng, "High-stiffness thermoplastic elastomer in hybrid soft actuator design for precision control," *Soft Robot.*, vol. 9, no. 3, pp. 456–468, 2022, [Online]. Available: https://doi.org/10.1089/soro.2021.0056

[133] Z. Chen, Y. Huang, and C. Lee, "3D printed PEBA-reinforced soft gripper with spatial accuracy optimization," *Addit. Manuf.*, vol. 41, p. 101961, 2021, [Online]. Available: https://www.sciencedirect.com/science/article/pii/S2214860421001480

[134] M. Luo, Y. Tan, and H. Zhao, "Multi-material soft actuator with PEBA for enhanced positional accuracy and reduced lateral deflection," *Adv. Intell. Syst.*, vol. 2, no. 10, p. 2000111, 2020, [Online]. Available: https://doi.org/10.1002/aisy.202000111

[135] S. Li, Y. Chen, and C. Majidi, "Hybrid-material integration in soft robotic fingers for enhanced shape adaptability and mechanical robustness," *IEEE Trans. Robot.*, vol. 37, no. 4, pp. 1257–1270, 2021, [Online]. Available: https://ieeexplore.ieee.org/document/9392453

[136] P. Polygerinos, N. Correll, and G. M. Whitesides, "Design of multi-material actuators for bioinspired soft robots: balancing flexibility and force," *Adv. Funct. Mater.*, vol. 29, no. 23, p. 1900371, 2019, [Online]. Available: https://doi.org/10.1002/adfm.201900371

[137] J. Shintake, E. Piskarev, and R. F. Shepherd, "Soft pneumatic actuators with integrated stiffness control using material zoning strategies," *Sci. Robot.*, vol. 5, no. 43, p. eaaz6894, 2020, [Online]. Available: https://www.science.org/doi/10.1126/scirobotics.aaz6894

[138] Y. Yang, Z. Chen, and T. Wang, "Bioinspired multi-material soft grippers with adaptive stiffness and selective actuation," *Soft Robot.*, vol. 9, no. 6, pp. 1121–1132, 2022, [Online]. Available: https://doi.org/10.1089/soro.2021.0061

[139] A. Zolfagharian, A. Kaynak, and S. Choi, "Multi-material 4D printing of soft actuators: Design and modeling of functionally distributed stiffness," *Mater. Des.*, vol. 192, p. 108709, 2020, [Online]. Available: https://www.sciencedirect.com/science/article/pii/S0264127519310859

[140] A. Miriyev, K. Stack, and H. Lipson, "Functionally graded soft actuators for bioinspired robotic motion control," *Nat. Commun.*, vol. 12, p. 1492, 2021, [Online]. Available: https://www.nature.com/articles/s41467-021-21732-3